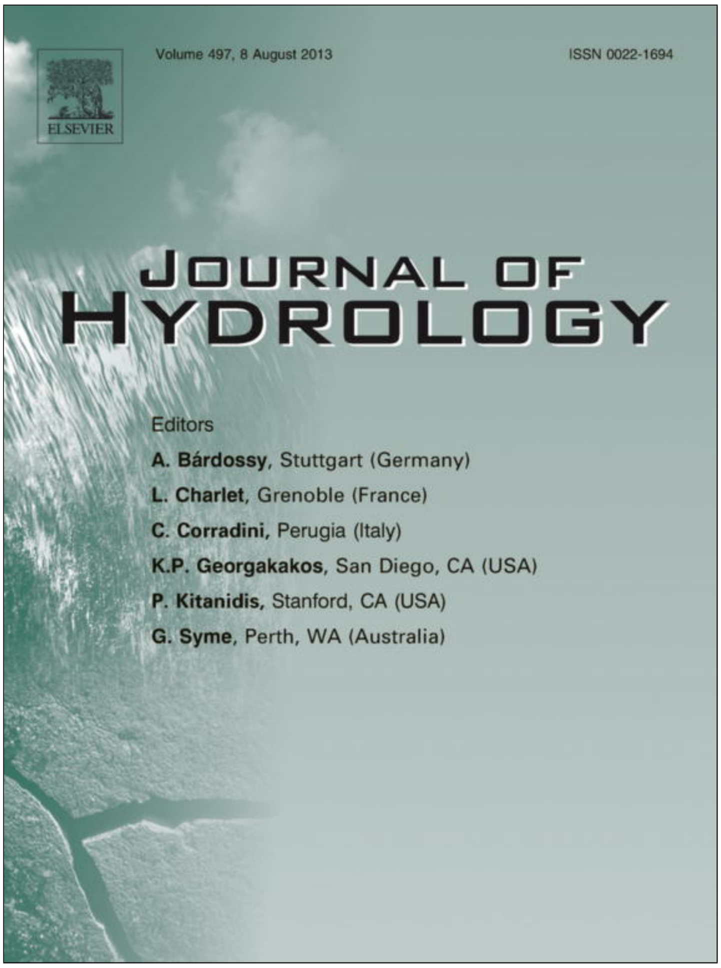
Volume 497, 8 August 2013
ISSN 0022-1694
ELSEVIER
JOURNAL OF HYDROLOGY
Editors
A. Bárdossy, Stuttgart (Germany)
L. Charlet, Grenoble (France)
C. Corradini, Perugia (Italy)
K.P. Georgakakos, San Diego, CA (USA)
P. Kitanidis, Stanford, CA (USA)
G. Syme, Perth, WA (Australia)

Journal of Hydrology 497 (2013) 145–151

Contents lists available at SciVerse ScienceDirect

Journal of Hydrology

journal homepage: www.elsevier.com/locate/jhydrol

Comparison of Stefan model with Single-phase model of water infiltration process in unsaturated porous media (theory and experiment)

Seksan Suttisong, Phadungsak Rattanadecho *, Prempreeya Montienthong

Center of Excellence in Electromagnetic Energy Utilization in Engineering (CEEE), Department of Mechanical Engineering, Faculty of Engineering, Thammasat University (Rangsit Campus), Pathumthani 12120, Thailand

ARTICLE INFO

Article history:
Received 16 December 2011
Received in revised form 23 May 2013
Accepted 30 May 2013
Available online 11 June 2013
This manuscript was handled by Corrado Corradini, Editor-in-Chief

Keywords:
Water infiltration
Moving boundary
Single-phase flow
Porous media

SUMMARY

Stefan models have been used for many problems such as freezing and melting processes. However, there are few research reports on using Stefan model for the problem of unsaturated flow in a granular packed bed, but the Stefan model has never been used before for considering the effects of particle sizes and supplied water flux to water saturation and moving infiltration fronts. The purpose of this work is to present novel mathematical models and numerical schemes for solving one-dimensional infiltration flow problems. A systematic development and comparison of two proposed models (Single-phase model and Stefan model) is performed. The influences of particle sizes and supplied water flux on water infiltration, i.e., the infiltration layer are studied in detail. It is found that the results of the comparison between these two models are in good agreement. Furthermore, the Stefan model shows better agreement with the experimental results than the Single-phase model. This study shows that the Stefan model can be used effectively for many physical phenomena involving flow infiltration coupled with a moving boundary, compared with other conventional models, i.e., the Single-phase model.

1. Introduction

Water infiltration is an important process in many fields, such as hydrology, soil science, agriculture, civil engineering, and chemical engineering. The infiltration characteristics of water are of prime interest for a variety of concerns, including water conservation, flooding, runoff, erosion, recovery of isothermal energy, temperature control of soil, and food preservation processes. The infiltration of water is affected by several intrinsic and extrinsic factors. The intrinsic factors that affect water infiltration are the hydraulic conductivity function, water retention characteristics, porosity, capillary pressure gradient, and texture of media.

The models of water infiltration in unsaturated porous media have been studied by many researchers. Abriola and Pinder (1985) proposed an infiltration model of porous media contamination by organic compounds. They considered the effects of the matrix and fluid compressibility, phase composition and the mechanism of driving forces, i.e., capillarity, diffusion and dispersion on flow phenomena in porous media. Stauffer and Dracos (1986) presented an experimental and numerical study of water and solute infiltration in layered porous media, which was restricted to two-dimensional flow in a vertical plane. They highlighted the relation between capillary pressure and the degree of saturation. Haverkamp et al. (1977) compared the numerical simulation models for one-dimensional infiltration. They reported that the implicit or explicit evaluation of the hydraulic conductivity and water capacity functions appear to have the widest range of applicability for predicting water movement in soil with both saturated and unsaturated regions. Other reviews concerning the problem of mass transport in porous media have been performed by Aoki et al. (1991), Ma et al. (2010), Henry and Smith (2006), Binning and Celia (1999), Parlange (1972), Gvirtzman et al. (2008), Ratanadecho et al. (2001, 2002), and Suttisong and Rattanadecho (2011).

Most previously proposed models of water infiltration in porous media have used conventional numerical methods to solve the nonlinear equations. Few studies (Broadrige et al., 2009; Borsi et al., 2004) that have been proposed modeling water infiltration in porous media based on the moving boundary model, or the "Stefan model", owing to the complexity of handling both the flow phenomena and the variation over time of the moving infiltration front. Stefan models have been used for many problems concerning the moving boundary condition, such as the freezing or thawing of soil, ice formation, crystal growth, aerodynamic ablation, casting of metal, food processing and numerous others. Generally, the solution of the moving boundary problem with phase transition has been of special interest because of the inherent difficulties associated both with the nonlinearity of the interface conditions and

* Corresponding author. Tel.: +66 0 2564 3001 9; fax: +66 0 2564 3010.
E-mail address: ratphadu@engr.tu.ac.th (P. Rattanadecho).

0022-1694/$ - see front matter © 2013 Elsevier B.V. All rights reserved.
http://dx.doi.org/10.1016/j.jhydrol.2013.05.048

Nomenclature

s	water saturation (–)
s_e	effective water saturation (–)
s_{ir}	irreducible water saturation (–)
ρ_p	density of particle (kg/m^3)
ρ_l	density of water (kg/m^3)
ε	porosity (–)
$F_{l,in}$	supplied water flux (kg/m^2 s)
g	gravity (m^2/s)
K	saturated hydraulic conductivity (m^2)
K_{rl}	relative permeability
υ_l	fluid velocity (m/s)
p_c	capillary pressure (Pa)
p_l	fluid pressure (Pa)
p_g	gas pressure (Pa)
μ_l	dynamic viscosity of liquid (Pa s)
υ_l	kinematic viscosity (m^2/s)
σ	surface tension (N/m)
η	coordinate tranformation

Subscripts

s	solid
l	liquid
p	particle

with the unknown locations of the arbitrary moving boundaries. The advantage of the Stefan model is that it is able to handle the moving boundary front in the various kinds of engineering problems, mentioned above. Crank and Gupta (1975) provide a good introduction to the Stefan problems and elaborate a collection of numerical methods. Lyczkowski and Chao (1984) present a comparison of the Stefan model with a two-phase model of a coal drying process in Cartesian and axisymmetric cylindrical coordinates. Javierre et al. (2006) report on the exciting numerical techniques for solving one-dimensional Stefan problems in phase transformation problems. To date, the related problems of Stefan models have been investigated by many researchers: Charn-Jung and Kaviany (1992), Chellaiah and Viskanta (1988), Crowley (1978), Shamsundar and Sparrow (1976), Cheung et al. (1984), Weaver and Viskanta (1986), Afshar and Shobeyri (2010), Saeedpanah et al. (2011), Rattanadecho (2004a,b, 2006), and Rattanadecho and Wongwises (2007). They have introduced various numerical techniques in attempting to overcome the difficulties in handling these moving boundary problems.

Although Stefan models have been used for many problems, relatively few researches report on the problem of unsaturated flow in a granular packed bed based on a Stefan model. In particular, the effects of particle sizes and supplied water flux on water infiltration in porous media and on the infiltration front have never been studied before. The purpose of this work is to: (1) solve numerically the two models (Single-phase model and Stefan model) for describing the one-dimensional infiltration of water in porous media; (2) compare the predicted results obtained for the two models; and (3) compare the predicted results obtained from these two models with the experimental results. The results presented here provide a basis for the fundamental understanding of infiltration flow in porous media.

2. Theory and numerical schemes

The mathematical models derived from mass conservation and Darcy's laws based on Buckley–Leverett function are performed. The main transport mechanisms that enable water infiltration of supplied water into a porous media, i.e., a granular packed bed are water flow driven by the capillary pressure gradient and gravity. Subsequently, a comparison is undertaken of the water infiltration process in unsaturated porous media, between the Single-phase model and the Stefan model.

2.1. Single-phase model

By conservation of mass in the unsaturated porous media, the governing equation of infiltration flow can be derived by using the volume averaged technique (Rattanadecho, 2004a,b).

The main assumptions involved in the formulations of the transport model are:

1. The unsaturated granular packed bed is rigid.
2. No chemical reactions occur in the granular packed bed.
3. Darcy's law holds for the liquid phase.
4. Gravity is included for the flow analysis.
5. Permeability of liquid can be expressed in terms of relative permeability.

Fig. 1 shows a schematic diagram of the Single-phase model or Buckley–Leverett problem. This is an unsaturated flow of water, supplied uniformly at the top surface of a granular packed bed, which is initially composed of glass particles and voids with uniform porosity throughout.

In this study, it is noted that the supplied water flux during unsaturated flow is considered to be lower than the supplied water flux owing to gravity (Aoki et al., 1991), namely:

$$F_l \leqslant g \cdot K \tag{1}$$

where F_l is the supplied water flux, g is the gravity and K is the saturated hydraulic conductivity (permeability). This expression means that the supplied water always infiltrates into the granular packed beds throughout the infiltration process.

2.1.1. Mass conservation

Regarding the infiltration flow in a granular packed bed, the microscopic mass conservation equation for liquid flow in such a packed bed is expressed as:

$$\varepsilon \frac{\partial}{\partial t}[\rho_l s] + \frac{\partial}{\partial z}[\rho_l \upsilon_l] = 0 \tag{2}$$

where ε is the porosity, s is the water saturation, ρ_l is the density of water, υ_l is the fluid velocity. The generalized Darcy's law, which is the expression for the superficial average velocity of the liquid phase, is defined as (Rattanadecho, 2002):

$$\upsilon_l = -\frac{KK_{rl}}{\mu_l}\left[\frac{\partial p_g}{\partial z} - \frac{\partial p_c}{\partial z} - \rho_l g\right] \tag{3}$$

where K_{rl} is the relative permeability, p_g is the gas pressure and μ_l is the liquid viscosity. In Eq. (3), the capillary pressure, p_c is related to the liquid and gas phases which can be written as:

$$p_c = p_g - p_l \tag{4}$$

where p_l is the liquid pressure and p_g is the gas pressure. Using Darcy's generalized equation (Eq. (3)), the mass conservation equation for the Single-phase model (Eq. (2)) can then be rewritten in its final form as:

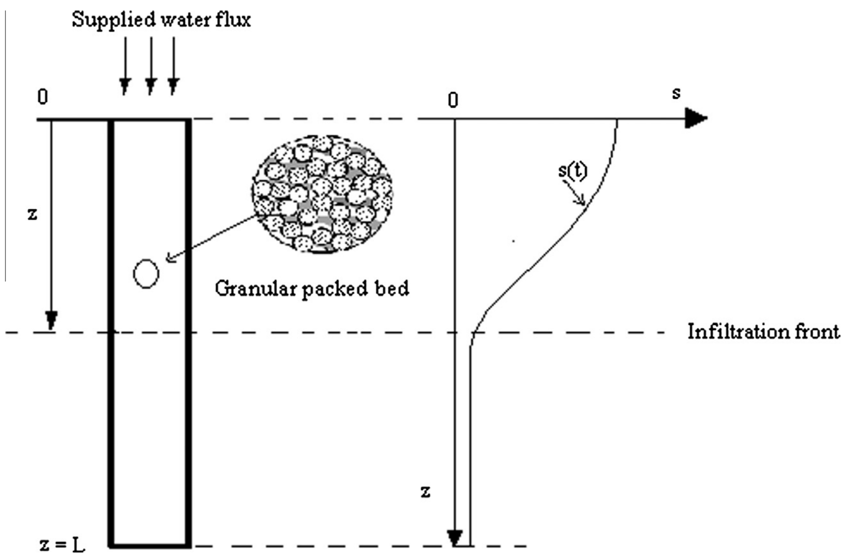

Fig. 1. Schematic representation of the water infiltration in porous media described by the Single-phase model.

$$\varepsilon\frac{\partial}{\partial t}[\rho_l s] - \frac{\partial}{\partial z}\left[\frac{KK_{rl}}{\upsilon_l}\left(\frac{\partial p_g}{\partial z} - \frac{\partial p_c}{\partial z} - \rho_l g\right)\right] = 0 \tag{5}$$

where υ_l is the kinematic viscosity. Assuming the effect of gas pressure is negligible, Eq. (5) is reduced to:

$$\varepsilon\frac{\partial}{\partial t}[\rho_l s] + \frac{\partial}{\partial z}\left[\frac{KK_{rl}}{\upsilon_l}\left(\frac{\partial p_c}{\partial z} + \rho_l g\right)\right] = 0 \tag{6}$$

2.1.2. Equilibrium relations

The system of conservation equations obtained for the Single-phase transport model requires a constitutive equation for the relative permeability, K_{rl}, capillary pressure, p_c, and capillary pressure functions (Buckley–Leverett functions), J. A typical set of constitutive relation for liquid system is given by:

$$K_{rl} = s_e^3 \tag{7}$$

where s_e is the effective water saturation, considered as the irreducible water saturation, s_{ir}, which can be defined by:

$$s_e = \frac{s - s_{ir}}{1 - s_{ir}} \tag{8}$$

The relation between relative permeability in each phase following Eq. (8) is shown in Fig. 2.

Furthermore, the capillary pressure, p_c, is further assumed to be represented adequately by Buckley–Leverett's well known $J(s_e)$

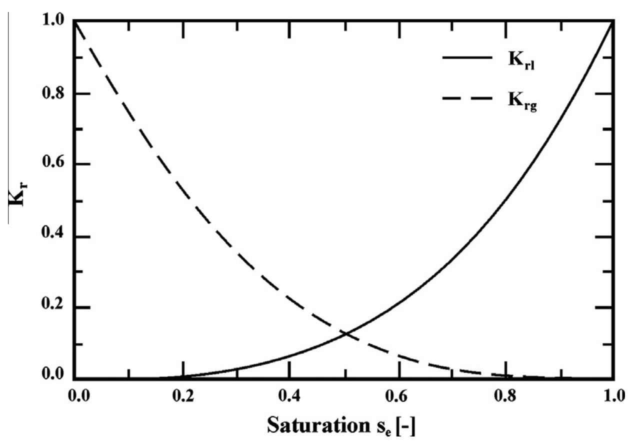

Fig. 2. The relationship between, K_r and s_e.

functions. The relation between the capillary pressure and the water saturation is defined by using the Buckley–Leverett functions, $J(s_e)$ Rattanadecho et al., 2002:

$$p_c = p_g - p_l = \frac{\sigma}{\sqrt{K/\varepsilon}}J(s_e) \tag{9}$$

where σ is the surface tension and $J(s_e)$ is correlated to capillary pressure data obtained by Buckley–Leverett and can be expressed as follows (Aoki et al., 1991):

$$J(s_e) = 0.325(1/s_e - 1)^{0.217} \tag{10}$$

2.1.3. Initial condition and boundary conditions

Assuming that the initial effective water saturation and initial temperature are constant and uniform throughout the granular packed bed:

$$t < 0, \quad z \geqslant 0 : s_e = s_0, \quad T = T_0 \tag{11}$$

Based on experimental conditions, the initial effective water saturation s_e is given as $s_0 = 0.001$ and the initial temperature T_0 is given as $T_0 = 25$ °C. The boundary conditions at the top and bottom of granular packed bed are:

$$\begin{aligned} &t > 0, \quad z = 0 : F_{l,in} = const, \\ &z = L : F_{l,out} = \rho_l \upsilon_l \end{aligned} \tag{12}$$

2.2. Stefan model

Fig. 3 shows a schematic diagram representing the water infiltration in a granular packed bed, as described by the Stefan model. This is one of the more powerful models that can solve the problems involved with the moving boundary, i.e., the infiltration front in this study, because it can simultaneously capture directly the infiltration front together with the infiltration layer during the water infiltration process in porous media.

The study of the water infiltration process in a granular packed bed based on the Stefan model is difficult because the interface between the wet and dry zones, or the infiltration front, is moving from the top of the granular packed bed to the bottom. For solving this moving boundary problem, the original governing equations are transformed into the coordinate transformation equations, which are based on a boundary fixing method. Refer to the original equations (Eqs. (6), (11), and (12)), as shown again below:

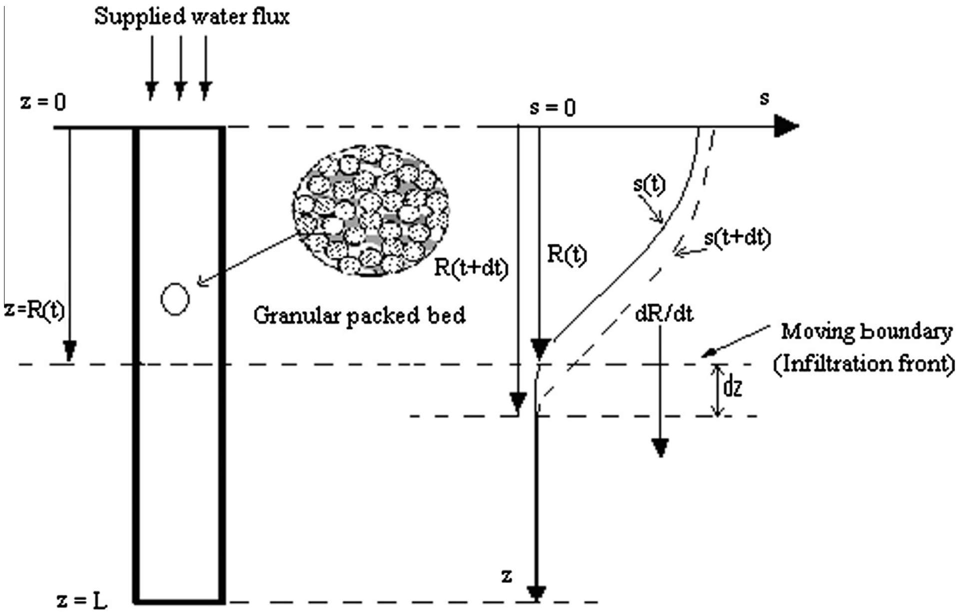

Fig. 3. Schematic representation of the water infiltration in porous media described by the Stefan model.

$$\varepsilon\frac{\partial}{\partial t}[\rho_l s]+\frac{\partial}{\partial z}\left[\frac{KK_{rl}}{\upsilon_l}\left(\frac{\partial p_c}{\partial z}+\rho_l g\right)\right]=0 \tag{6}$$

$$t<0,\quad z\geqslant 0: s_e=s_0,\quad T=T_0 \tag{11}$$

$$\begin{aligned}&t>0,\quad z=0: F_{l,in}=const,\\&z=L: F_{l,out}=\rho_l\upsilon_l\end{aligned} \tag{12}$$

Considering the moving boundary front or water infiltration front, when the mass balance in performed at this interface, the equation representing the infiltration front (Stefan equation) is described by:

$$\varepsilon s\frac{\partial R}{\partial t}=\frac{KK_{rl}}{\mu_l}\left(\frac{\partial P_c}{\partial z}+\rho_l g\right) \tag{13}$$

With the concept of coordinate transformation technique, the following normalized form is applied (Rattanadecho 2004a):

$$\eta=z/R(t),\quad 0\leqslant z\leqslant R(t) \tag{14}$$

as shown in Fig. 3, where $R(t)$ is the distance between the top surface ($z = 0$), and the moving boundary front ($z = R(t)$). For a time step, the infiltration front moves in the z direction. At the moving boundary front ($z = R(t)$), the initial effective water saturation s_e is given as $s_0 = 0.001$. By using the coordinate transformation technique, the physical space (z, t) is then transformed to the mapping space [$\eta(z, t)$, t]. The differential operators with the coordinate transformation are mathematically related to the following equations (Rattanadecho 2004a):

$$\frac{\partial}{\partial z}=\frac{\partial}{\partial\eta}\frac{\partial\eta}{\partial z}=\frac{1}{R}\frac{\partial}{\partial\eta} \tag{15}$$

$$\frac{\partial}{\partial t}=\frac{\partial}{\partial\eta}\frac{\partial\eta}{\partial t}+\frac{\partial}{\partial t}=\frac{\partial}{\partial t}-\frac{\eta\dot{R}}{R}\frac{\partial}{\partial\eta} \tag{16}$$

where $\dot{R}$ is the time derivative of the water infiltration front. Finally, Eq. (6) in coordinate transformation form is rewritten as (Rattanadecho 2004a):

$$\varepsilon\left(\frac{\partial}{\partial t}-\frac{\eta\dot{R}}{R}\frac{\partial}{\partial\eta}\right)[\rho_l s]+\frac{1}{R}\frac{\partial}{\partial\eta}\left[\frac{KK_{rl}}{\upsilon_l}\left(\frac{1}{R}\frac{\partial p_c}{\partial\eta}+\rho_l g\right)\right]=0 \tag{17}$$

Eq. (13) in coordinate transformation form is also rewritten as:

$$\varepsilon s\left(\frac{\partial R}{\partial t}-\frac{\eta\dot{R}}{R}\frac{\partial R}{\partial\eta}\right)=\frac{KK_{rl}}{\mu_l}\left(\frac{1}{R}\frac{\partial P_c}{\partial\eta}+\rho_l g\right) \tag{18}$$

2.3. Numerical schemes

Corresponding to the method of finite differences, based on the notion of control volume, the generalized systems of nonlinear equations with a coordinate transformation form are integrated over a typical computational domain. These equations within this system can be cast into a numerical discretization of the generalized conservation equation. To solve the nonlinear equations, the Newton–Raphson iteration procedure is used for each element. After integration over each control volume within the computational mesh, a system of nonlinear equation results whereby each equation can be cast into a numerical discretization of the generalized conservation equation.

The Single-phase model (Eq. (6)) for the internal nodes can be cast into a numerical discretization as:

$$\begin{aligned}&\frac{\varepsilon}{\Delta t}(1-s_{ir})\left(\rho_l\left(s_{ei}^{n+1}-s_{ei}^{n}\right)\right)+\frac{1}{\Delta z}\left(\rho_l\left(\frac{KK_{rl}}{\mu_l}\bigg|_{i+\frac{1}{2}}\left(\frac{P_{ci+1}^{n+1}-P_{ci}^{n+1}}{\Delta z}+\rho_l g\right)\right.\right.\\&\left.\left.-\frac{KK_{rl}}{\mu_l}\bigg|_{i-\frac{1}{2}}\left(\frac{P_{ci}^{n+1}-P_{ci-1}^{n+1}}{\Delta z}+\rho_l g\right)\right)\right)=0\end{aligned} \tag{19}$$

The Stefan model (Eq. (17)) can be cast into a numerical discretization as:

$$\begin{aligned}&\frac{\varepsilon}{\Delta t}(1-s_{ir})\left(\rho_l\left(s_{ei}^{n+1}-s_{ei}^{n}\right)\right)-\frac{n\dot{R}}{R}(1-s_{ir})\left(\rho_l\left(s_{ei}^{n+1}-s_{ei}^{n}\right)\right)\\&+\frac{1}{R\Delta\eta}\left(\rho_l\left(\frac{KK_{rl}}{\mu_l}\bigg|_{i+\frac{1}{2}}\left(\frac{P_{ci+1}^{n+1}-P_{ci}^{n+1}}{R\Delta\eta}+\rho_l g_z\right)\right.\right.\\&\left.\left.-\frac{KK_{rl}}{\mu_l}\bigg|_{i-\frac{1}{2}}\left(\frac{P_{ci}^{n+1}-P_{ci-1}^{n+1}}{R\Delta\eta}+\rho_l g_z\right)\right)\right)=0\end{aligned} \tag{20}$$

where n is the current iteration index and $n + 1$ is the new iteration index. The discretized form of the moving boundary interface in Eq. (18) can be written as:

$$\varepsilon s \frac{3R^{n+1} - 4R^n + R^{n-1}}{2\Delta t} = \frac{KK_{rl,i+1} + KK_{rl,i}}{2\mu_l} \left(\frac{P_{c,i+1} - P_{c,i}}{R\Delta\eta} + \rho_l g \right) \tag{21}$$

Finally, to obtain values for all stage variables at the matching time, the system of nonlinear equations (Eqs. (19–21)) must be resolved by the Newton–Raphson method.

3. Experimental apparatus

Fig. 4 shows the experimental apparatus for the one-dimensional water infiltration in a granular packed bed (Aoki et al., 1991). The test column is designed to achieve the one-dimensional flow of infiltrating water. It has an inner diameter of 60 mm, is 400 mm long and is made of rigid acrylic plastic tubing. The dry porous-ceramic disk at the bottom of the granular packed bed support the granular particles in the column while allowing air to escape in advance of the infiltration front. A thick plug of insulation is also placed again the ceramic disk at the bottom of the column. Spherical soda lime glass beads with average sizes (d) of 0.15 and 0.4 mm, are used as a sample of the granular packed bed. The water is supplied (supplied water flux, f) from a water tank to the top surface of the granular packed bed through a distributor with controlled rates of 0.05 and 0.1 kg/m^2 s. The test column is covered with insulation.

The position of the infiltration depth in the packed bed is captured by digital camera relative to a time-based reference, as shown in Fig. 4. At the end of the test run, the granular packed bed is cut into five sections, each with volume of 183 cm^3, in order to measure the water saturation. The water saturation in the non-hygroscopic porous packed bed was defined as the fraction of the volume occupied by water to the volume of the pores. This water saturation was obtained by weighing the dry and wet mass of the sample. Before the experiment, each section was weighed individually to record its dry mass. The porous packed bed was weighed again at 5 min after the test run. The water saturation formula can be described in the following form (Rattanadecho, 2004a and Aoki et al., 1991):

$$s = \frac{\rho_p \cdot (1 - \varepsilon) \cdot (m_w - m_d)}{\rho_l \cdot \varepsilon \cdot m_d} \tag{22}$$

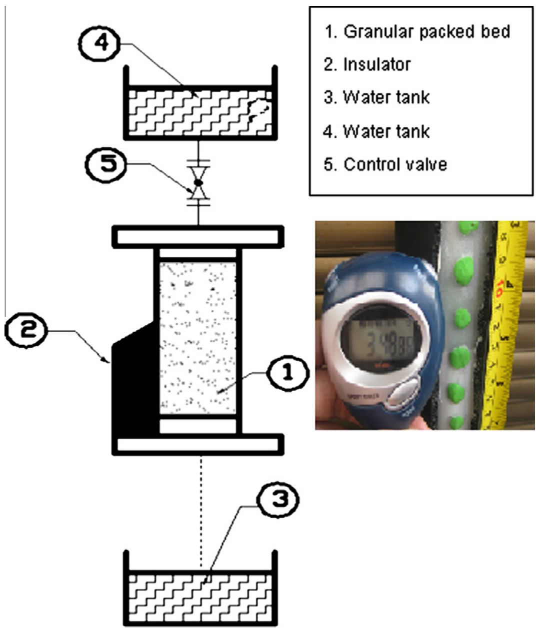

Fig. 4. Experimental apparatus for measuring unsaturated flow in one dimension porous layered.

where s is water saturation, ρ_p is the density of the particles, ρ_l is the density of water, ε is porosity, and m_w and m_d are the wet and dry mass of the sample, respectively.

4. Results and discussion

In this study, the numerical results of a Single-phase model and a Stefan model are described for the one-dimensional infiltration of water in porous media. The numerical results between the Stefan model and Single-phase model are carried out in this study. Subsequently, these numerical results are compared with the experimental results. The effects of particle size (d) and supplied water flux (f) on water infiltration, i.e., the infiltration layer and the infiltration front are studied in detail.

Fig. 5 shows the comparison of the progress of the infiltration layer through the granular packed bed (d = 0.15 mm) between the two models at various elapsed times, as a parameter of supplied water flux (f = 0.05 kg/m^2 s and 0.1 kg/m^2 s). It is evident that the infiltration layer or water distribution can be regarded as a parameter of the supplied water flux. Greater supplied water flux results in a faster infiltration rate and forms a wider infiltration layer with time. The main transport mechanisms that enable fluid movement in porous media are liquid flow driven by capillary pressure gradient and gravity, as mentioned in Eq. (3). The predicted infiltration layers in both models are in good agreement, especially in the case of the lower supplied water flux. This is because the movement of the infiltration front is not as fast for the case of lower supplied water flux where no difference of computing performance of these two models has been found. Nevertheless, for the case of the higher supplied water flux, the differences of predicted results obtained from both models are clearly shown. In contrast with the case of the lower supplied water flux, the movement of the infiltration front for the case of the higher supplied water flux is faster owing to the hydrodynamic characteristics. In this case, the difference between the computing performances of these two models is clearly evidenced. The com-

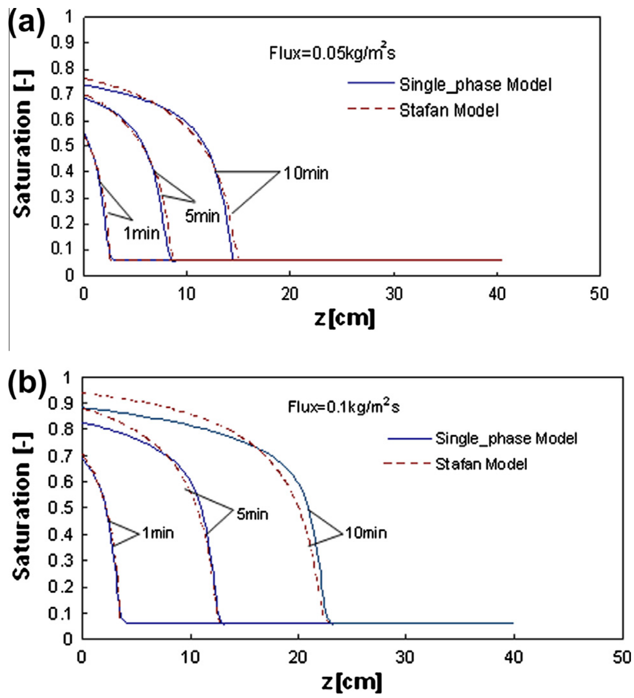

Fig. 5. Comparison of infiltration layer along granular packed bed (d = 0.15 mm) between two models at various elapsed times as a parameter of supplied water flux: (a) f = 0.05 kg/m^2 s and (b) 0.1 kg/m^2 s.

puting performance from the both models will be discussed again in the following paragraphs.

Figs. 6 and 7 show the influences of the supplied water flux and particle sizes on the infiltration layer for the two models. The larger particle size and greater supplied water flux results in a faster infiltration rate and forms a wider infiltration layer in the granular packed bed. The effect of the fast response depends on hydrodynamic characteristics, i.e., capillary pressure gradient, permeability and gravity.

Fig. 8 shows the comparison of the infiltration front ($d = 0.15$ mm and $d = 0.4$ mm) between the two models as a parameter of the supplied water flux ($f = 0.05$ kg/m^2 s and 0.1 kg/m^2 s). Numerically, it is observed that for all testing cases, the predicted results obtained from both models are in good agreement, especially in the case of the lower supplied water flux, mentioned with regard to Fig. 5. This means that the proposed calculation technique based on the Stefan model is appropriate for modeling flow infiltration, especially in the case of sensitively moving boundary front.

Fig. 9 shows the comparison of the infiltration layer through the granular packed bed with different particle sizes between the numerical results and the experimental result ($t = 5$ min and $f = 0.1$ kg/m^2 s). It is evident that the predicted results from both models are in agreement with the experimental results. Furthermore, the numerical results based on the Stefan model seem to be nearer the experimental results than do those of the Single-phase model in the case of sensitively moving boundary fronts. This is because the Stefan model can solve accurately the problems involved with the moving boundary, because it can simultaneously capture directly the moving front together with the infiltration layer during the water infiltration process in a granular packed bed. However, the conventional method, i.e., the Single-phase model, aims to predict the saturation profile or infiltration layer, but it cannot capture directly the moving front and infiltration layer at the same time.

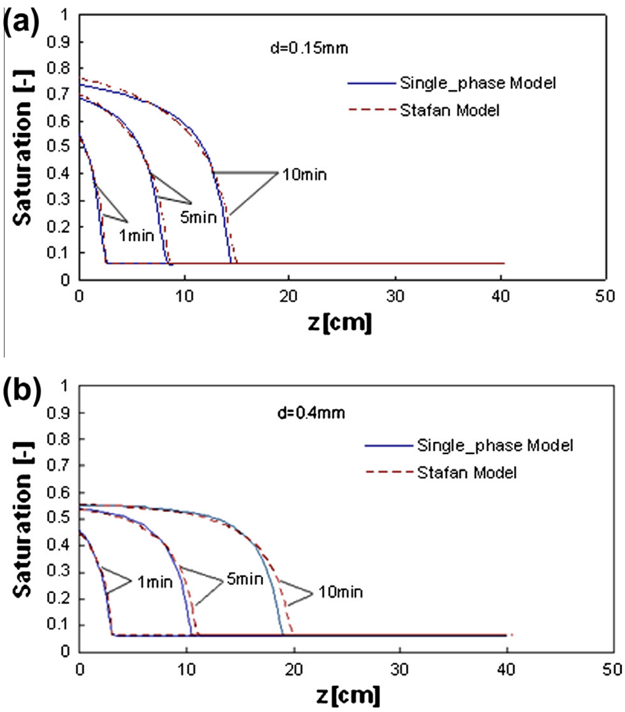

Fig. 6. Comparison of infiltration layer along granular packed bed ($f = 0.05$ kg/m^2 s) between two models at various elapsed times as a parameter of particle sizes: (a) $d = 0.15$ mm and (b) 0.4 mm.

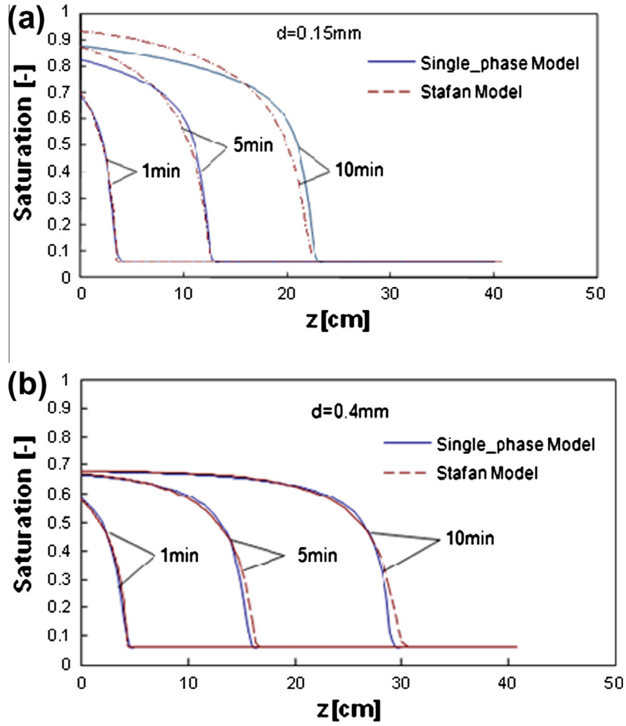

Fig. 7. Comparison of infiltration layer along granular packed bed ($f = 0.1$ kg/m^2 s) between two models at various elapsed times as a parameter of particle sizes: (a) $d = 0.15$ mm and (b) 0.4 mm.

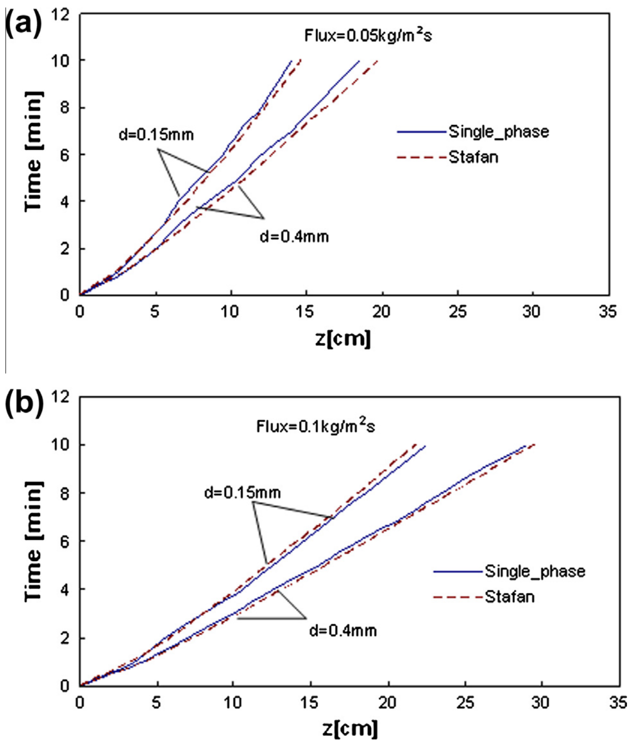

Fig. 8. Comparison of infiltration front ($d = 0.15$ mm and $d = 0.4$ mm) between two models as a parameter of supplied water flux: (a) $f = 0.05$ kg/m^2 s and (b) 0.1 kg/m^2 s.

Again, these results confirm that the troublesome numerical errors in the conventional method (Eqs. (2–12) and (19): Single-phase model) are reduced effectively if the solution procedure is linked with the discontinuities condition and if a special formula

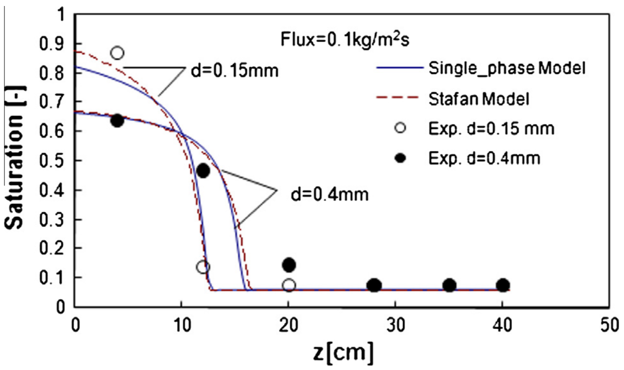

Fig. 9. Comparison of infiltration layer along granular packed bed with different particle size between numerical results and experimental result ($t = 5$ min, $f = 0.1$ kg/m^2 s).

is used to incorporate the jump conditions directly into the numerical model (Eqs. (14–18), (20) and (21): Stefan model). This is the main idea behind this work in considering the moving boundary as a prior parameter, because the water infiltration process is the moving boundary problem that involve infiltration front. Even though, the Stefan model seems more accurate than that Single-phase model, the relative computation times are slightly higher than for performing the calculation using the Single-phase model because of the greater memory usage. This issue needs to be improved in further research.

5. Conclusions

Water infiltration in a granular packed bed with unsaturated flow is investigated numerically using the Single-phase and the Stefan models. The results show that for all test cases the predicted results obtained from both models are in good agreement. Furthermore, the predicted results obtained from these two models are also in good agreement with the experimental results. The proposed calculation technique, based on the Stefan model is appropriate for modeling the flow infiltration process, especially in the cases of a sensitively moving boundary front. Furthermore, the larger particle size and a greater supplied water flux in the granular packed bed correspond to a faster infiltration flow, compared with smaller particle size and a lower supplied water flux. Gravity and capillary pressure are shown clearly to have an influence on the infiltration flow.

Acknowledgement

This work was supported by Thailand Research Fund (TRF).

References

Abriola, M., Pinder, F., 1985. A multiphase approach to the modeling of porous media contamination by organic compounds 1. Equation development. Water Resources Research 21, 11–18.
Afshar, M.H., Shobeyri, G.R., 2010. Efficient simulation of free surface flows with discrete least-squares meshless method using a priori error estimator. International Journal of Computation Fluid Dynamics 24 (9), 349–367.
Aoki, K., Hattori, M., Kitamura, M., Shiraishi, N., (1991). Characteristics of heat transport in porous media with water infiltration. ASME/JSME Thermal Engineering Proceeding 4, 303–308.
Binning, Philip, Celia, Michael A., 1999. Practical implementation of the fractional flow approach to multi-phase flow simulation. International Journal of Advances in Water Resources 22, 461–478.
Borsi, I., Farina, A., Fasano, A., 2004. On the infiltration of rain water through the soil with runoff of the excess water. Nonlinear Analysis: Real World Applications 5, 763–800.
Broadrige, P., Triadis, D., Hill, J.M., 2009. Infiltration from supply at constant water content: an integrable model. Journal of Engineering Mathematics 64, 193–206.
Charn-Jung, K., Kaviany, M., 1992. Numerical method for phase-change problems with convection and diffusion. International Journal of Heat and Mass Transfer 35, 457–467.
Chellaiah, S., Viskanta, R., 1988. Freezing of saturated and superheated liquid in porous media. International Journal of Heat and Mass Transfer 31, 321–330.
Cheung, F.B., Chawla, T.C., Pedersen, D.R., 1984. The effect of heat generation and wall interaction on freezing and melting in finite slab. International Journal of Heat and Mass Transfer 27, 29–37.
Crank, J., Gupta, R.S., 1975. Isotherm migration method in two dimensions. International Journal of Heat and Mass Transfer 18, 1101.
Crowley, A.B., 1978. Numerical solution of Stefan problems. International Journal of Heat and Mass Transfer 21, 215.
Gvirtzman, Haim., Shalev, Eyal., Dahan, Ofer., Hatzor, Yossef.H., 2008. Large-scale infiltration experiments into unsaturated stratified loess sediment: monitoring and modeling. International Journal of Hydrology 349, 214–229.
Haverkamp, R., Vauclin, M., Touma, J., Wierenga, P.J., Vanchaud, G., 1977. A comparison of numerical simulation models for one-dimension infiltration. Soil Sci. Soc. Am. J. 41, 285–294.
Henry, E.J., Smith, J.E., 2006. Numerical demonstration of surfactant concentration-dependent capillarity and viscosity effects on infiltration from a constant flux line source. International Journal of Hydrology 329, 63–74.
Javierre, E., Vuik, C., Vermolen, F., 2006. A comparison of numerical models for one-dimensional Stefan problems. Journal of Computational and Applied Mathematics 2006 (192), 445–459.
Lyczkowski, R.W., Chao, Y.T., 1984. Comparison of Stefan model with two-phase model of coal drying. International Journal of Heat and Mass Transfer 27, 1157–1169.
Ma, Ying., Feng, Shaoyuan., Dongyuan, Su., Gao, Guangyao, Huo, Zailin, 2010. Modeling water infiltration in a large layered soil column with a modified Green-Ampt model and HYDRUS-1D. Int. J. Computer and Electronics in Agriculture 71S, S40–S47.
Parlange, J.Y., 1972. Theory of water movement in soils: one-dimensional infiltration. Soil Science 111, 170–174.
Ratanadecho, P., Aoki, K., Akahori, M., 2001. Experimental and numerical study of microwave drying in unsaturated porous material. International Communications in Heat and Mass Transfer 28, 605–616.
Ratanadecho, P., Aoki, K., Akahori, M., 2002. Influence of irradiation time, particle sizes and initial moisture content during microwave drying of multi-layered capillary porous materials. ASME Journal of Heat Transfer 124, 151–161.
Rattanadecho, P., 2004a. Experimental and numerical study of solidification process in unsaturated granular packed bed. Journal of Thermophysics and Heat Transfer 18, 87–93.
Rattanadecho, P., 2004b. Theoretical and experimental investigation of microwave thawing of frozen layer using a microwave oven (effects of layered configurations and layer thickness). International Journal of Heat and Mass Transfer 47, 937–945.
Rattanadecho, P., 2006. Simulation of melting of ice in a porous media under multiple constant temperature heat sources using a combined transfinite interpolation and PDE methods. Chemical Engineering Science 61, 4571–4581.
Rattanadecho, P., Wongwises, S., 2007. Moving boundary-moving mesh analysis of freezing process in water-saturated porous media using a combined transfinite interpolation and PDE mapping methods. ASME Journal of Heat Transfer 31, 318–333.
Saeedpanah, I., Jabbari, E., Shayanfar, M.A., 2011. Numerical simulation of ground water flow via a new approach to local radial point interpolation meshless method. International Journal of Computation Fluid Dynamics 24 (1), 17–30.
Shamsundar, N., Sparrow, E.M., 1976. Effect of density change on multi-dimensional conduction phase change. ASME Journal of Heat Transfer 105, 550.
Stauffer, F., Dracos, T., 1986. Experimental and numerical study of water and solute infiltration in layered porous media. Journal of Hydrology 84, 9–34.
Suttisong, S., Ratanadecho, P., 2011. The experimental investigation of heat transport and water infiltration in granular packed bed due to supplied hot water from tom top: influence of supplied water flux, particle sizes and supplied water temperature. Experimental and Thermal Fluid Science. http://dx.doi.org/10.1016/j.expthermflusci.2011.07.003.
Weaver, J.A., Viskanta, R., 1986. Freezing of liquid-saturated porous media. ASME Journal of Heat Transfer 108, 654–659.